Adsorption equilibrium, kinetics, and thermodynamics assessment of the removal of the reactive red 141 dye using sesame waste

Hojatolah Sohrabi, Elham Ameri*

*Department of Chemical Engineering, Shahreza Branch, Islamic Azad University, P.O. Box 311-86145, Shahreza, Iran,
Tel. +98 321 3292242, ext. 6341; Fax: +98 265 2423898; emails: hojatsohrabi2009@gmail.com (H. Sohrabi),
ameri@iaush.ac.ir (E. Ameri)*

ABSTRACT

Adsorption of the reactive red 141 dye from aqueous solutions onto sesame hull waste, as a kind of useless agricultural waste, in a batch process was studied. The biosorbent was characterized by scanning electron microscope and Fourier transform infrared spectroscopy. There were hydroxyl groups, carboxyl groups, etc. on the surface of the sorbent, as shown by Fourier transform infrared spectroscopy. Adsorption was investigated as a function of the particle size, the amount of adsorbent, the pH, the initial dye concentration, and the agitation speed with time. The maximum removal of dye molecules was found to be 95% at pH 1.1, the initial dye concentration of 30 mg L^{-1}, the adsorbent dose of 4 g L^{-1}, and the temperature of 20°C. The experimental equilibrium data were analyzed, showing that the adsorption behavior of the reactive red dye could be described well reasonably by Langmuir isotherm model with the maximum sorption capacity of 27.55 mg g^{-1} for the biosorbent. Kinetics studies also revealed that the adsorption of the dye followed pseudo-second-order kinetics, with the regression, R^2, of 0.994. The adsorption process was exothermic with a mean change in the enthalpy of −15.48 kJ mol^{-1}, and spontaneous with a mean free energy change of −15.38 kJ mol^{-1}. Due to the exothermic nature of the adsorption process, the removal percentage of the dye was improved remarkably from 50% at the temperature of 323.15 K to over 70% at the temperature of 298.15 K. The acidic aqueous solution with the initial pH <2 favored the adsorption of the anionic reactive red dye by the sesame waste biosorbent (with pH$_{pzc}$ of 5.1). Through the reusability study of the sorbent, the removal percentages of dye were found to be 94, 91, 87, and 80% for 1st, 2nd, 3rd, and 4th cycles of adsorption, respectively.

Keywords: Agricultural waste; Biosorption; Isotherm; Reactive dye; Sesame

1. Introduction

Textile and other industries generally use dyes and pigments to color their products. The discharge of colored dye effluent into the environment interferes with the diffusion of the sunlight into waters, delays photosynthesis, and obstructs the growth of aquatic biota [1]. Moreover, a number of dyes are either toxic or mutagenic and carcinogenic [2]. Reactive dyes are highly dissolved in water media, according to their hydrophilic nature. This class of dyes is considered as harmful to aquatic life in rivers and sea, where they

*Corresponding author.

are released by several industries. Research on the toxicity of azo dyes such as reactive red 141 shows genotoxicity, mutagenicity, mortality, and carcinogenicity in experiments with aquatic fauna (fish, algae, bacteria, etc.) and also those carried out with mammals. Moreover, some research has reported the individual toxicity of the reactive red 141 dye manufactured from known carcinogens aromatic compounds such as naphthalene [3]. The mechanism of carcinogenicity involves the formation of acyloxy amines during N-hydroxylation and N-acetylation of the aromatic amines in azo dyes such as the reactive red 141 dye followed by O-acylation. These acyloxy amines can be converted to nitremium and carbonium ions that bind to DNA and RNA, causing to tumor formation and several kinds of mutations [4]. Therefore, due to the high toxicity of the reactive red141 dye, various adsorbents have been used for the removal of this type of reactive dye from its solutions [5,6].

Reactive dyes are one of the greatest well-known classes of dye stuffs generally used for cotton and other cellulosic materials, but they are also used to a limited extent on wool and nylon. They can be fixed to fabric by forming a covalent bond, which is a significant advantage over other classes of dyes. Therefore, such reactive dyes can be immobilized via mechanical entrapment or physical adsorption [7]. Numerous studies have described techniques for the removal of dyes from aqueous solutions using various treatment methods, including biological processes, combined chemical and biochemical processes, chemical oxidation, coagulation, adsorption, and membrane treatments. Reviewing the presented literature indicates that among the various investigated techniques, adsorption occupies a noticeable place in dye removal. This is probable owing to its simplicity and high level of effectiveness [8]. A number of natural and synthetic adsorbents have been considered for the removal of dyes from their solutions [9–11]. Among these adsorbents, activated carbon is one of the most extensively evaluated and used materials for environmental pollution control. The basic disadvantage of activated carbon is its high production and treatment costs [9,12]. Consequently, much attention has been focused on low-cost adsorbents such as natural materials, biosorbents, and waste materials from industry and agriculture for the removal of heavy metals ions and dye from water [11,13–17]. Moreover, industrial waste products (activated charcoal ash), animal waste materials (hen feather), agricultural wastes (wheat bran), and metal oxide nanoparticles (magnesium oxide nanoparticles) have been used as the sorbent for the removal of dyes from solution [5,11,18–22].

Moreover, various agricultural wastes have been investigated for the removal of several types of dyes. In this regard, sawdust has been used for the removal of dyes from water and wastewater [23]. This material is composed of cellulose, lignin, and hemicellulose, with polyphenolic groups playing a significant role in binding dyes through complexation, ion exchange, and hydrogen bonding mechanisms. Mittal and Kurup employed power plant waste material; bottom ash, and an agriculture waste product; de-oiled soya to remove a hazardous dye acid red-27. They reported the ability of the wastes in removing the acid red-27 dye from aqueous solutions in a fixed bed column [24]. Rice husk has been used by McKay et al. for the elimination of two basic dyes, safranine and methylene blue, and the adsorption capacities of 838 and 312 mg g^{-1} were reported, respectively [25]. Wool carbonizing has been studied by Perineau et al. for the adsorption of dyes [26]. Wheat husk, an agricultural byproduct, has been utilized by Gupta et al. for the removal of reactofix golden yellow 3 RFN from an aqueous solution [27]. Recently, Sharma et al. modified *Hibiscus cannabinus* fiber by graft copolymerization with vinyl monomer acrylic acid (AAc) and binary mixture of AAc and acrylamide. The modified *H. cannabinus* fibers were reported as the potential candidate for the removal of the dye from the aqueous system [28]. Moreover, Mittal et al. used bottom ash as an adsorbent to remove and recover a hazardous halogen-containing dye eosin yellow. During the batch studies, various parameters influencing the adsorption were considered. According to bulk removal, through column operation, about 97% of saturation of the dye was reported [29].

The hull part of sesame waste (SW) usually disposed in the environment causes the environmental pollution. Therefore, the conversion of SW to some low-cost biosorbents is performed to fulfill two goals in this work. First, the useless SW was converted to a beneficial material. Moreover, it could be efficiently used for the reduction of environmental pollution. In this work, we aimed to investigate the usability of SW for the adsorption of the reactive red 141 dye from aqueous solutions. During the experiments, the effects of several operational parameters such as the initial concentration of feed solution, contact time, adsorbent dose, adsorbent particle size, agitation speed, solution pH, and solution temperature were investigated. The adsorption kinetics, isotherm, and thermodynamics were studied to realize the adsorption mechanism of the reactive red dye onto the SW. At last, the desorption study was performed to regenerate the dye-loaded SW and subsequently to reuse the regenerated sorbent in the adsorption process.

2. Materials and method

2.1. Materials

The reactive red 141 dye was purchased from Sigma–Aldrich and used without purification. The characteristics of the dye are listed in Table 1. All chemicals used in the adsorption experiments were purchased from Merck and used without further purification.

2.2. Preparation of sesame biosorbent

SW (hull part) was collected from a local industry and washed thoroughly with distilled water to remove any dirt. It was dried in an oven at 110℃ and sieved to various mesh sizes, namely 30, 40, 50, 70, and 100 BSS mesh. The SW powder was characterized using Fourier transform infrared spectrometer (PE-1710, USA) in the range of 4,000–400 cm^{-1}. In this regard, the mixture of SW powder with KBr was ground and then pressed with a special press to provide a disk of standard diameter. The surface of SW was observed on a SEM-Stereo Scan LEO, Model-400 scanning electron microscope (SEM), before and after the biosorption.

Moreover, zero point charge (pH_{pzc}) was estimated for SW. Also, the BET (Brunauer, Emmett and Teller) surface area for SW was measured using Smart Sorbs 92 surface area analyzer.

2.3. Batch adsorption

Adsorption experiments were performed by shaking (IKA KS130Basic) a known amount of SW with 25 ml solution of the dye with the desired concentration in batch mode. The concentrations of the red dye ranged from 10 to 250 $mg\,L^{-1}$. The experiments were carried out at different pH values (1–11), dif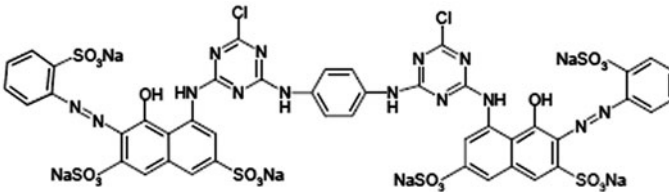ferent agitation speeds (80–640 rpm), and different amounts of biosorbent (0.05–2 g). The initial pH of the dye solution was adjusted by adding 0.1 N NaOH or HCl, using a Radwag Model AS 220/C/2 pH meter. The progress of biosorption was monitored at different time intervals till the achievement of equilibrium. After the completion of predetermined time intervals, the content of the beakers was centrifuged at 4,000 rpm (Nuve NF200). The negligible residue of the biosorbent in solution was removed by filter paper (Whatman 40). Concentrations of the dye solutions were measured at the characteristic wavelength ($\lambda_{max} = 530\,nm$) of the red dye using a UV–vis spectrophotometer (T70). From this data, the equilibrium adsorption capacity and the percentage removal of dye were calculated. Also, in order to estimate the adsorption capacity of SW, the experimental data were fitted to the Langmuir and Freundlich isotherm models. Moreover, to reveal the agreement of the isotherm models with the experimental results, the determination coefficient, R^2, was estimated.

Kinetic studies of SW were also performed at various concentrations of the red dye and accordingly the extent of adsorption was studied as a function of time. Kinetic experiments were carried out at 25℃. To calculate the thermodynamic parameters for the interaction of dye–sesame, the removal of the dye from solution by SW was conducted in a batch mode after 120 min of agitation at different temperatures, e.g. 20, 30, 40, and 50℃. According to the results achieved from some preliminary experiments, the adsorption isotherms, kinetic, and Thermodynamic studies were carried out at the pH 1.5, the initial dye concentration of 100 $mg\,L^{-1}$, the stirring speed of 240 rpm, and the adsorbent dose of 4 $g\,L^{-1}$.

2.4. Desorption studies

In order to perform the batch desorption study, 0.1 g of SW which had been used for the dye adsorption from the solution with the initial concentration of

Table 1
Details of reactive red 141 dye

Dye	Formula and molecular weight	λ_{max}	Structure
RR141	$C_{52}H_{26}Cl_2N_{14}O_{26}S_8Na_8$ 1,463	530 nm	

30 mg L^{-1} at the pH 1.1 was separated from the dye solution by centrifugation. The saturated SW was washed mildly with water to eliminate any unloaded dye. At that time, the washed SW was stirred using a magnetic stirrer with 25 ml of doubly distilled water, and 0.1 mol L^{-1} NaOH solution for 12 h, in the order mentioned. After that, the regenerated SW was dried and used in the dye adsorption process again. At last, the removal percentage of the dye was found, and desorption/adsorption process was repeated four times, according to the experimental conditions during the first stage.

3. Results and discussion

3.1. Characterization of the biosorbent

3.1.1. Scanning electron microscopy

The SEM images of the SW before and after dye uptake were obtained. SEM results of the unloaded SW showed that SW consisted of tiny particles with various sizes ranging from 0.471 to 2.539 μm, on average. Moreover, the SEM images of SW samples showed a considerable number of holes with a diameter ranging from 0.889 to 1.594 μm, where there was a good chance for dye molecules to be trapped and adsorbed into the empty and unfilled spaces. SEM images for the loaded SW showed that the interspaces between particles disappeared due to the surface coverage of SW. In the case of the dye-adsorbed SW, surface color was changed, possibly due to the adsorption of dye molecules on the surface coverage of SW.

3.1.2. Fourier transform infrared analysis of the biosorbent

The FTIR spectra analysis, before and after dye adsorbed SW, was achieved. The spectra of SW were measured in the wave number range of 400–4,000 cm^{-1}.

The FTIR spectrum of SW showed a broad peak at 3,489 cm^{-1} that could be assigned to the O–H stretching vibrations of cellulose, pectin, hemicellulose, and lignin [30]. The bands at 2,926 and 2,854 cm^{-1} were attributed to the stretching vibration of –CH$_3$ and–CH$_2$, respectively. A very strong peak at 1,744 cm^{-1} could be assigned to the C=O stretching vibration of carbonyl. The peak at 1,627 cm^{-1} could be attributed to the stretch vibration of C–C from the aromatic ring [31]. The peak at 1,463 cm^{-1} was representative of the symmetric bending of –CH$_3$. The peak which appeared at 1,375 cm^{-1} was due to the symmetric

stretching of –COO$^-$. The peaks at 1,031–1,316 were assigned to the C–O stretching of alcohol and carboxylic acids. Moreover, the band perceived at 1245 cm^{-1} was also assigned to the presence of the C–O stretching of phenols. After the loading of SW, the band shifting and the possible involvement of hydroxyl group were found to be represented as the broad peak at 3,489 cm^{-1}. In addition, a decrease in peak intensity at 3,507 cm^{-1} was due to the interaction between dye and different O–H groups in the SW. In this regard, Dolphen et al. implied that the hydroxyl group of chitin was the main functional group for reactive dye adsorption by covalent bonding [32]. Moreover, a new peak was appeared at 723 cm^{-1}. This peak might be assigned to C–Cl or S–O of the reactive dye, confirming the attachment of the dye on SW.

3.2. Equilibrium contact time and initial dye concentration

In order to achieve the equilibrium time for the maximum dye uptake onto SW, experiments were carried out in different contact times with a fixed adsorbent dose of 4 g L^{-1} for the solution with the initial concentration of 100 mg L^{-1}, the pH 1.5, and the shaking rate of 240 rpm. During the first 10 min of the adsorption process, the rate of the removal of dye was high and equilibrium was reached after 120 min (Fig. 1). Finally, after reaching the saturation to the value of 72%, a smooth graph was attained.

The reduction in the rate of dye extraction with time could be explained here. While a large number of unsaturated sites are available for adsorption during the initial stage, the remaining active sites are difficult to be filled owing to the repulsive forces between the
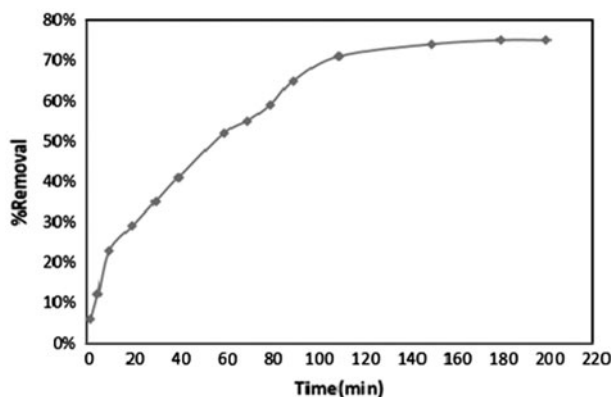

Fig. 1. The biosorption of the dye onto sesame as a function of time (the initial dye concentration of 100 mg L^{-1}, the agitation speed of 240 rpm, the adsorbent dose of 4 g L^{-1}, and the pH 1.5).
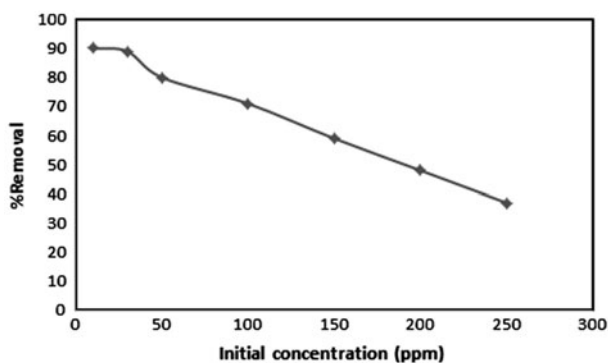
Fig. 2. The biosorption of the dye onto sesame at different initial metal concentrations (the agitation speed of 240 rpm, the adsorbent dose of 4 g L^{-1}, and the pH 1.5).
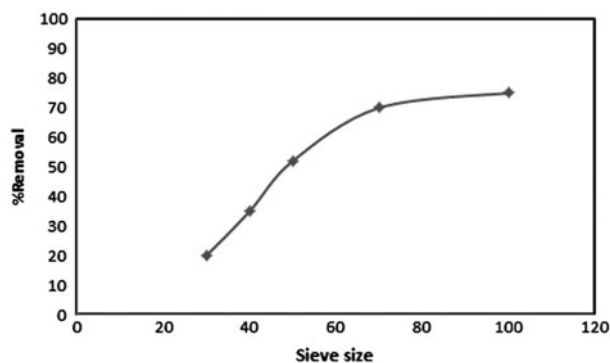

Fig. 3. The biosorption of the dye onto sesame using various mesh sizes of the biosorbent (the initial dye concentration of 100 mg L^{-1}, the agitation speed of 240 rpm, the adsorbent dose of 4 g L^{-1}, and the pH 1.5).

dye molecules on the biosorbent and on the solution with the passage of time [33].

Moreover, the dye molecules adsorbed into the available pores in the biosorbent get almost filled with dye during the initial stage of the adsorption process. Subsequently, the dye molecules have to go over farther and deeper into smaller pores fronting much larger resistance [34].

To determine the effect of the initial dye concentration on the adsorption process, the initial concentration of dye was changed from 10 to 250 mg L^{-1}. Batch adsorption experiments were performed at pH 1.5, with the adsorbent dose of 4 g L^{-1}, and the shaking rate of 240 rpm. From Fig. 2, it could be seen that the percentage of adsorption was reduced from 90 to 37% with an enhancement from 10 to 250 mg L^{-1} in the dye initial concentration. In this regard, Sulak and Yatmaz investigated the effect of the initial concentration of the reactive red 180 dye varying from 10 to 200 mg L^{-1} using wheat bran as the sorbent. They showed that increasing dye concentration decreased the adsorption efficiency at concentrations higher than 60 mg L^{-1}; the ideal dye concentration was decided to be 50 mg L^{-1} [22].

In general, the percentage of dye removal is declined with a rise in the initial dye concentration, possibly owing to the saturation of the active sites on the adsorbent [35]. At low concentrations, there can be unfilled active sites on the adsorbent surface, and when the initial dye concentration is enhanced, the active sites needed for dye adsorption may not be available [36].

3.3. The effect of particle size

Batch adsorption experiments were performed at different particle sizes, namely 30, 40, 50, 70, and

100 BSS mesh, the pH 1.5, the adsorbent dose of 4 g L^{-1}, and the shaking rate of 240 rpm. Fig. 3 displays that with the increase in the mesh size of biosorbent the rate of the adsorption was enhanced. This was based on the enhancement in the average mass transfer area of the adsorbent and the accessibility of the adsorbent pores toward the dye. Thereafter, the SW with the mesh size of 100 was chosen for the adsorption experiments based on the sufficient adsorption capacity. A similar result was obtained by other researchers. The effect of particle size on the removal of Cd(II) was studied using some sesame having particle sizes ranging from 0.15 to 2 mm, with the initial concentration of 20 mg L^{-1}. It was shown that the removal of Cd(II) was improved with a reduction in particle size, and milling to a particle size of 210 μm for sesame seemed to be suitable for adsorption [16].

3.4. The effect of agitation rate

The agitation speed varied from 80 to 640 rpm. The experiments were carried out at the pH 1.5, the initial dye concentration of 100 mg L^{-1}, and the adsorbent dose of 4 g L^{-1}. The results showed (Fig. 4) that the sorption capacity of SW for the dye was enhanced with an increase in the agitation speed from 80 to 480 rpm.

Moreover, removal percentages of the reactive red dye were achieved to be 45, 71, and 82 for 80, 240, and 480 rpm agitation speeds, respectively. From these data, one could conclude that the rate of dye removal was considerably increased with an enhancement in the agitation rate with values up to 240 rpm, and then it was slightly enhanced for the shaking rates over 480 rpm. The increase in the adsorption with the
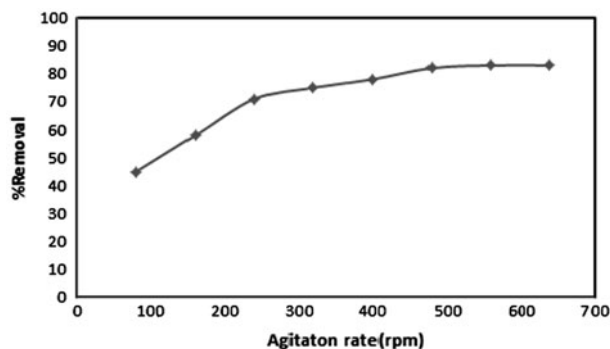
Fig. 4. The biosorption of the dye onto sesame at different agitation speeds (the initial dye concentration of $100\ mg\ L^{-1}$, the adsorbent dose of $4\ g\ L^{-1}$, and the pH 1.5).

Fig. 5. The biosorption of the dye onto sesame at different pH values (the initial dye concentration of $100\ mg\ L^{-1}$, the agitation speed of 240 rpm, and the adsorbent dose of $4\ g\ L^{-1}$).

increase in the agitation speed was probably due to an enhancement in the mobility of the sorbing species. Moreover, this effect could be attributed to the enhancement in turbulence and the reduction in boundary layer thickness around the sorbent particles as a result of the increase in the agitation rate.

This result was also in agreement with the findings obtained by Azizi and Ameri for the adsorption of lead ions onto magnetic wheat straw, and those reported by Elkady et al. for the adsorption of dye onto egg shell too [17,37]. For example, an investigation in to the agitation dependence of the dye biosorption process by Elkady et al. evidenced that the percentage of dye sorption was significantly improved from 32 to 60% as the agitation speed was enhanced from 100 to 500 rpm, and then it remained constant at the higher agitation rate. They elucidated that the influence of external diffusion on the sorption kinetic control played a noteworthy role. However, the effect of agitation speed seemed to be negligible at high agitation rates [37].

3.5. The effect of solution's pH and biosorbent dose

To investigate the effect of pH, the adsorption of dye molecules was studied with the adsorbent dose of $4\ g\ L^{-1}$, the initial ion concentration of $100\ mg\ L^{-1}$, and the shaking rate of 240 rpm. The variation in the biosorption of the reactive red dye was investigated in the pH range of 1.1–11. The results are displayed in Fig. 5.

It is clear from the plot that the reduction of the solution pH led to an enhancement in the biosorption of the dye onto the sesame biosorbent. The removal percentage of the dye was improved remarkably from 5% at the pH 5 to over 71% at the pH 1.1. It was noticeable that through pH variation from 5 to 11, the
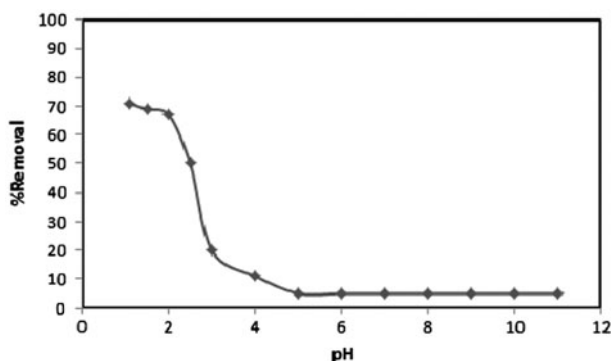
dye removal percentage was not changed and remained constant. The same performance was reported for the adsorption of various textile dyes on the agricultural waste [38,39]. The ionic forms of the dye in solution and the surface electrical charge of the biosorbent are related to the solution pH. So, the interaction between the dye and adsorbent is generally affected by ionization states of the functional groups on both dye molecules and adsorbent surface [40]. The improvement of dye uptake at acidic pH values may be referred to electrostatic interactions between the SW and the reactive red dye. In this regard, Sakkaya-wong et al. showed that under acidic conditions, electrostatic interaction occurred between the protonated amine, acetamide in chitin as a biosorbent and sulfonate (SO_3^-) group of the reactive red 141 dye as an adsorbate [41]. Moreover, this could be explained in terms of the value of pH_{pzc} obtained for the sesame biosorbent (see Fig. 6) and the molecular form of the dyes at each pH considered. Generally, the adsorption
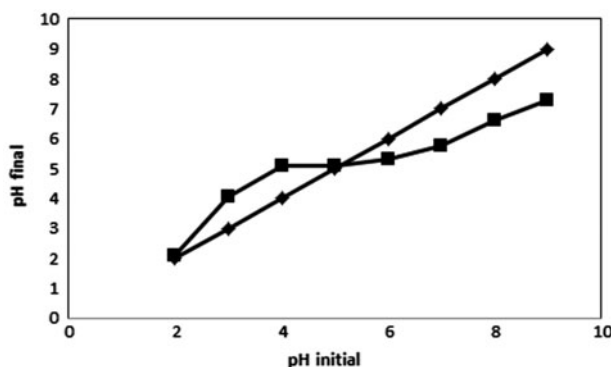

Fig. 6. Plot for determination of point zero charge of the sesame.

of anions was favored at $pH < pH_{PZC}$, whereas the pH_{PZC} value was found to be 5.1 for SW biosorbent. At $pH \geq pH_{pzc}$, it was found that the electrostatic repulsion between the negatively charged dye molecules (sulfonate groups) and the negatively charged surface of the sesame biosorbent led to reduction in the biosorption of dyes onto the biosorbent. So, as the pH of the solution was increased beyond 2, the dye adsorption was diminished considerably and the dye adsorbed on SW was maximum at the pH 1.1.

Based on present results, the pH value of 1.1 for the reactive red dye was reported as the optimized value. A similar result has been stated by Vieira et al. in the investigation of the adsorption of blue remazol R160 onto babassu coconut mesocarp. The pH_{PZC} for the babassu coconut mesocarp was found to be 6.7, while the maximum capacity of blue remazol R160 adsorption was at pH 1.1 [42]. Moreover, orange peel waste was used by Namasivayam et al. for the adsorption of congo red, procion orange and rhodamine B dyes. The process was performed at different pHs, showing that acidic pH was favorable for the adsorption for all three dyes [43].

The effect of the biosorbent dose on the removal of the reactive red dye from the solutions of the initial concentration of 100 mg L^{-1} is shown in Fig. 7. Experiments were performed with different amounts of adsorbent (0.05–2.0 g), at the pH 1.5 and the shaking rate of 240 rpm.

As expected, increasing the dose of biosorbent led to improvements in the biosorption of the dye onto SW. In this regard, cereal chaff was used for the removal of methylene blue from aqueous solutions. The results indicated that as the dose of chaff was increased, the percentage of methylene blue sorption was improved too [44].
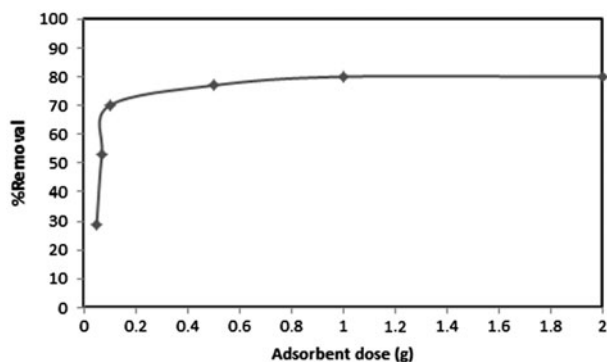

Fig. 7. The biosorption of the dye onto sesame using various biosorbent doses at (the initial dye concentration of 100 mg L^{-1}, the agitation speed of 240 rpm, and the pH 1.5).

It could also be seen that the reactive red dye removal was increased up to a certain limit and then remained almost constant. The trend could be attributed to the availability of more interaction sites. Moreover, the behavior observed for adsorption with dosage values beyond 1 could be due to the formation of adsorbent agglomerates which decreased the available average mass transfer area and blocked some of the adsorption sites. So, the optimum dosage of SW was found to be 40 g L^{-1} for the dye solution with the initial concentration of 100 mg L^{-1}. A similar trend has been reported for the removal of remazol red using eggshell as the adsorbent. It was shown that the removal of remazol red 198 was increased up to a maximum value and then remained constant. The optimum biosorbent dosage was found to be 10 g of egg shell per liter of dye solution [37].

3.6. Adsorption isotherms

Adsorption isotherm offers significant models in the explanation of the adsorption behavior. It describes how the adsorbate interacts with the adsorbent and provides a description of the nature and the mechanism of the adsorption process. While the adsorption reaction reaches equilibrium, the adsorption isotherm could distinguish the distribution of adsorbate molecules between the solid and the liquid phases. Hence, it is necessary to find the most appropriate correlation of equilibrium curves to optimize the conditions for designing adsorption systems. In the present work, the batch experiments were performed by adding a fixed amount of adsorbent (100 mg) to a series of glass flasks filled with 25 mL of dye solutions (1–150 mg L^{-1}) at the pH 1.5. The isotherm results were analyzed using the Langmuir and Freundlich isotherms.

The Langmuir adsorption model is based on the assumption that maximum adsorption relates to a saturated monolayer of solute molecules on the surface of adsorbent, without any lateral interaction between the adsorbed molecules. The linearized form of Langmuir equation is expressed as follows:

$$\frac{C_e}{q_e} = \frac{1}{Q_{max}b} + \frac{C_e}{Q_{max}} \tag{1}$$

where C_e is the equilibrium concentration (mg L^{-1}), q_e is the amount adsorbed at equilibrium (mg g^{-1}), and b (L mg^{-1}) and Q_{max} (mg g^{-1}) are Langmuir constants related to the energy of adsorption and adsorption capacity, respectively. The values of b and Q_{max} can

Table 2
Langmuir and Freundlich isotherm constants for reactive red 141 dye biosorption onto SW

Langmuir isotherm	Q_{max} (mg g^{-1})	b (L mg^{-1})	R^2
	27.55	0.019	0.99
Freundlich isotherm	K_F (L g^{-1})	$1/n$	R^2
	3.043	0.467	0.95

be determined from the slopes and the intercepts of the linear plots of C_e/q_e against C_e (Fig. 8). The values of R^2, b, and Q_{max} are presented in Table 2 from the Langmuir isotherm.

From data presented in Table 2, the adsorption capacity of SW for the removal of the reactive red 141 was obtained to be 27.55 mg g^{-1}. In order to find the performance of the SW for the reactive red 141 uptakes, it was necessary to compare its adsorption capacity to that for other biosorbents. Various adsorbents have been used for the removal of several types of dye. For example, peanut hull, coir pith, banana pith, and orange peel have been used to adsorb some different kinds of dyes, and their adsorption capacity has been found to be 13.99, 1.6, 4.42, and 19.88 mg g^{-1}, respectively [2,45–47]. Moreover, other types of the sorbents, such as Zn_2SnO_4 and metal hydroxide sludge, have been investigated for the removal of the reactive red 141 (anionic) dye with the maximum adsorption capacities of 56.18 and 61 mg g^{-1}, respectively [5,48].

So, by reviewing different research works, it could be inferred that there is a potential to utilize the SW as a low cost and also available sorbent to remove the reactive red 141 from aqueous solutions.

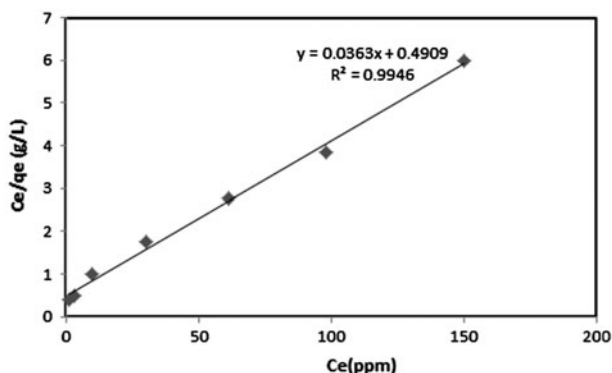In addition, by studying research works, it could be concluded that the adsorption capacities for cationic dyes adsorption were more than those for anionic dyes adsorption on the same biosorbents [45]. Since the carboxyl group is one of the main functional groups in agricultural wastes, it will influence the adsorption capacity due to the dye class. The carboxyl group with the negative charge inhibits the adsorption of the anionic dyes. Conversely, it favors the adsorption of the cationic dyes [2].

The Freundlich adsorption isotherm is another most widely applied isotherm that considers heterogeneous adsorptive energies on the adsorbent surface. A linear form of the Freundlich equation is expressed as follows:

$$\ln q_e = \ln K_F + \frac{1}{n} \ln C_e \qquad (2)$$

where q_e is the amount of dye adsorbed per unit mass of adsorbent at equilibrium (mg g^{-1}), C_e is the equilibrium concentration (mg L^{-1}), K_F is the Freundlich adsorption constant associated to the adsorption capacity of the adsorbent (mg L$^{-1/n}$ L$^{1/n}$ g^{-1}), and n (dimensionless) is used to describe the amount of adsorption and the adsorption intensity between the dye concentration and the adsorbent, respectively. The values of K_F and n were determined from the intercept and the slope of the plot of ln q_e vs. ln C_e. Fig. 9 displays the Freundlich plot. The isotherm parameters obtained from Freundlich plot are listed in Table 2.

It can be perceived from Table 2 that Langmuir model was best fitted to the empirical data with the coefficient of determination, R^2, being 0.9946, as represented in Fig. 8. This showed that SW would provide monolayer and homogeneous adsorption for the dye molecules.

In addition, the dimensionless constant separation factor or equilibrium parameter, R_L, can be evaluated using the following equation:

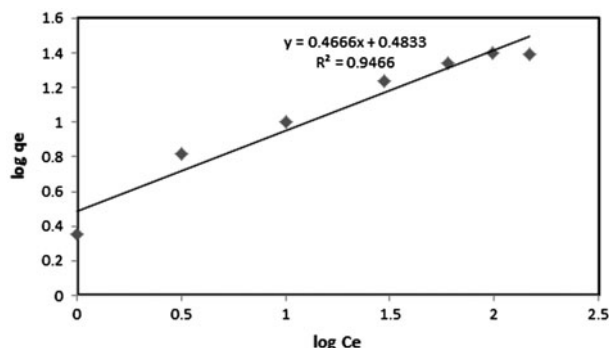Fig. 8. The biosorption isotherm of dye based on the Langmuir model.

Fig. 9. The biosorption isotherm of dye based on the Freundlich model.

$$R_L = \frac{1}{(1 + bC_o)} \qquad (3)$$

The value of the essential characteristics of the Langmuir isotherm, R_L (0.345), was between 0 and 1, indicating the favorable adsorption for SW used in this work.

3.7. Thermodynamic study

Experiments were performed to find the optimum temperature and calculate thermodynamic parameters on the adsorption of dye molecules onto SW at four different temperatures ranging from 298.15 to 323.15 K. The results are represented in Table 3.

The data presented in Table 3 showed that the value of the dye adsorbed was dropped as the temperature was raised. This observation indicated that the adsorption process was an exothermic one. This phenomenon could be due to the tendency of dye molecules to be released from the biosorbent to the aqueous solution with an increase in temperature. A similar result was also reported in an adsorption investigation of Cd(II) using SW as the biosorbent [15].

The thermodynamic parameters achieved for the adsorption system were calculated using the following equations. The values are represented in Table 3.

$$k'_c = C_{ad,e}/C_e \qquad (4)$$

$$\Delta G^\circ = -RT \ln k'_c \qquad (5)$$

$$\ln k'_c = \frac{-\Delta H^\circ}{RT} + \frac{-\Delta S^\circ}{R} \qquad (6)$$

where k'_c represents the apparent equilibrium constant of the biosorption, C_e is the equilibrium concentration (mg L^{-1}), $C_{ad,e}$ is the concentration of the adsorbate on the biosorbent at the equilibrium (mg L^{-1}), T is the temperature (K), and R is the gas constant. The value of k'_c was substituted in the next equation to achieve the change of Gibbs free energy of adsorption (ΔG°). Subsequently, the values of thermodynamic parameters such as change in enthalpy (ΔH°) and change in entropy (ΔS°) were determined using the van't Hoff equation (Eq. (6)). Plotting $\ln k'_c$ against $1/T$ gives a straight line with a slope and intercept equal to $\Delta H^\circ/R$ and $\Delta S^\circ/R$, respectively.

The results presented in Table 3 indicated that the magnitudes of Gibbs free energy nearly remained constant and were close to 15.38 kJ mol^{-1} during the adsorption process. The negative values of free energy showed that the dye adsorption onto SW was spontaneous. It should be noted that free energy values attained for the dye were diminished with increasing the temperature. The negative values of the enthalpy also indicated the exothermic nature of the adsorption, whereas the negative values of the entropy change showed reduced randomness at the solid/solution interface with some structural changes in the adsorbate and the adsorbent. The low value of ΔS° also pointed to the fact that no significant changes happened on entropy. Similar results have been reported by Elkady et al. who applied eggshell biocomposite beads for the adsorption of remazol reactive red 198 from aqueous solution [37]. They reported that the negative values of both the enthalpy and Gibbs free energy changes showed the exothermic as well as feasible and spontaneous nature of the biosorption process, respectively. They also found that the negative value of entropy change (−4.11 J mol^{-1}K^{-1}) indicated a reduced disorder at the solid/liquid interface during adsorption. Moreover, the value of ΔG° for the biosorption of the reactive red 180 onto wheat bran varied from −4.79 to −2.57 kJ mol^{-1} [22]. It was concluded from this data that the negative and small value of free energy change was indicative of the spontaneous nature of the biosorption process. The negative values of ΔH° as well as that of ΔS° also suggested the exothermic nature and the possibility of the favorable biosorption of the process, respectively [22].

Table 3
The effect of the temperature on the removal of the reactive red 141 dye, and thermodynamic parameters (the initial dye concentration of 100 mg L^{-1}, the pH 1.5; the stirring speed of 240 rpm and the adsorbent dose of 4 g L^{-1})

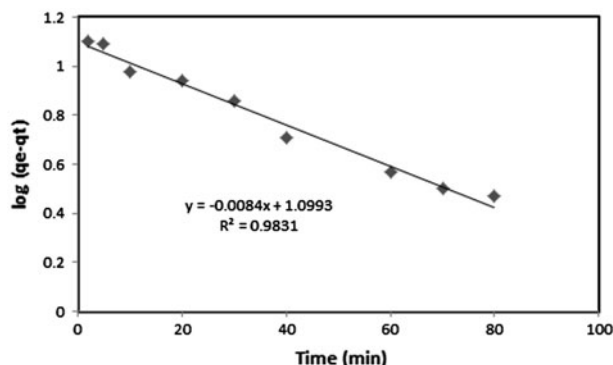| T (K)	% Removal	ΔG (kJ/mol)	ΔH (kJ/mol)	ΔS (kJ/mol)
298.15	70	−15.387	−15.482	−0.326
303.15	62	−15.384		
313.15	55	−15.380		
323.15	50	−15.377		

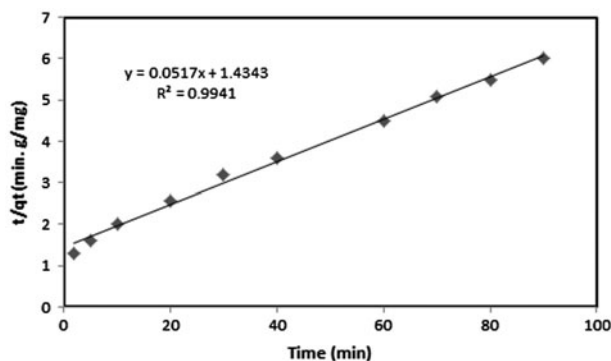Fig. 10. Pseudo-first-order biosorption kinetics of dye onto sesame.

Fig. 11. Pseudo-second-order biosorption kinetics of dye onto sesame.

3.8. Kinetic study

Kinetics is significant for the adsorption studies because it can calculate the rate at which a pollutant is removed from aqueous solutions and offers valuable data for distinguishing the mechanism of sorption reactions. In order to study the rate constant of the reactive red dye–SW system, two kinetics models were tested. The kinetic data were initially fitted with the first-order rate expression given as:

$$\ln(Q_e - Q_t) = \ln Q_e - k_1 t \tag{7}$$

where Q_t (mg g^{-1}) is the amount of metal ions biosorbed at time t, Q_e is the amount of metal ions biosorbed at equilibrium (mg g^{-1}), and k_1 is the rate constant of the biosorption (min^{-1}). Linear plot of ln $(Q_e - Q_t)$ vs. t for different adsorbent dosages should give a straight line if first-order kinetics is appropriate, and Q_e and k_1 can be estimated from the intercept and the slope of the plot, respectively. The linear plot of ln $(Q_e - Q_t)$ vs. t for the pseudo-first-order kinetic model is presented in Fig. 10, using SW.

The pseudo-second-order kinetic model is given by the expression:

$$\frac{t}{Q_t} = \frac{1}{k_2 Q_e^2} + \frac{t}{Q_e} \tag{8}$$

where Q_t and Q_e (mg g^{-1}) are the amounts of biosorption at time t (min) and equilibrium, respectively; k_2 (g mg^{-1} min^{-1}) is the rate constant of the second-order equation.

Fig. 11 shows pseudo-second-order plot for the adsorption process. k_2 and Q_e values were obtained from the intercepts and the slope of the linear plot, respectively.

The values of correlation coefficients (Table 4) for SW adsorbent showed a better fit of pseudo-second-order model with the experimental data with respect to the Lagergren first-order model, so one could conclude that the rate-limiting step was of chemisorption nature.

In this regard, bottom ash and hen feather as the biosorbents were tested for the removal of dyes, showing that the kinetic studies followed the pseudo-second-order model [18,29].

3.9. Dye desorption

Desorption experiments were carried out to explain the possibility of the recovery of the biosorbent. In order to display the reusability of the adsorbents, adsorption–desorption cycles of dye were repeated four times by reusing the test adsorbents. It could be perceived from this data that the removal percentages of dye were found to be 94, 91, 87, and

Table 4
Characteristic parameters of the kinetic models via coefficients of determination of reactive red 141 dye adsorption on SW

Pseudo-first-order		Pseudo-second-order	
R^2	$k \times 10^3$ (min^{-1})	R^2	$k \times 10^3$ (mg^{-1} g min^{-1})
0.983	8.4	0.994	1.864

80% for 1st, 2nd, 3rd, and 4th cycles of adsorption, respectively.

As a result, realizing the good adsorption capacity of 27.55 mg g^{-1} using SW and also achieving 80% dye removal efficiency using regenerated SW after the 4th cycle of desorption suggest that SW can be a suitable and useful biosorbent for the removal of the reactive red 141 dye from aqueous solutions at commercial level.

4. Conclusions

The efficiency of SW in removing the reactive red 141 dye from aqueous solutions was studied. Adsorption was influenced by various parameters such as the initial dye concentration, the agitation speed, the dosage and size of adsorbent, the solution temperature, and the initial pH. The maximum uptake of the dye by the SW occurred at an initial pH 1.1 and the adsorption was decreased with increasing dye concentration from 10 to 250 mg L^{-1}. A higher removal percentage of dye could be achieved at the higher agitation speed and adsorbent dosage, and with the lower size of adsorbent particles and temperature. The biosorption of the reactive red dye onto the SW was found to show a nonlinear favorable biosorption behavior that could be characterized well by the Langmuir isotherm model in the studied concentration range. It was shown that the kinetics of adsorption followed pseudo-second-order kinetics. Thermodynamic parameters revealed that the adsorption was spontaneous and exothermic. The desorption study showed that the SW could be used as an economical and suitable adsorbent to remove the reactive red 141 dye from aqueous solutions. Since SW is simply accessible in the countryside, it has the potential to be utilized for small-scale industries which discharge dyes into their effluent.

References

[1] J.H. Weisburger, Comments on the history and importance of aromatic and heterocyclic amines in public health, Mutat. Res. 506–507 (2002) 9–20.

[2] R. Gong, Y. Ding, M. Li, C. Yang, H. Liu, Y. Sun, Utilization of powdered peanut hull as biosorbent for removal of anionic dyes from aqueous solution, Dyes Pigm. 64 (2005) 187–192.

[3] S. Vinitnantharat, W. Chartthe, A. Pinisakul, Toxicity of reactive red 141 and basic red 14 to algae and waterfleas, Water Sci. Technol. 58 (2008) 1193–1198.

[4] M.A. Brown, S.C. De Vito, Predicting azo dye toxicity, Crit. Rev. Environ. Sci. Technol. 23 (1993) 249–324.

[5] E.L. Foletto, G.C. Collazzo, M.A. Mazutti, S.L. Jahn, Adsorption of textile dye on zinc stannate oxide: Equilibrium, kinetic and thermodynamics studies, Sep. Sci. Technol. 46 (2011) 2510–2516.

[6] W. Li, Q. Yue, P. Tu, Z. Ma, B. Gao, J. Li, X. Xu, Adsorption characteristics of dyes in columns of activated carbon prepared from paper mill sewage sludge, Chem. Eng. J. 178 (2011) 197–203.

[7] J.I. Kroschwitz, M. Howe-Grant, Kirk-Othmer Encyclopedia of Chemical Technology, Wiley publications, New York, NY, 1993.

[8] R. Han, D. Ding, Y. Xu, W. Zou, Y. Wang, Y. Li, L. Zou, Use of rice husk for the adsorption of congo red from aqueous solution in column mode, Bioresour. Technol. 99 (2008) 2938–2946.

[9] G. Crini, Non-conventional low-cost adsorbents for dye removal: A review, Bioresour. Technol. 97 (2006) 1061–1085.

[10] Z. Aksu, Application of biosorption for the removal of organic pollutants: A review, Process Biochem. 40 (2005) 997–1026.

[11] I. Özbay, U. Özdemir, B. Özbay, S. Veli, Kinetic, thermodynamic, and equilibrium studies for adsorption of azo reactive dye onto a novel waste adsorbent: Charcoal ash, Desalin. Water Treat. 51 (2013) 6091–6100.

[12] J.M. Dias, M.C.M. Alvim-Ferraz, M.F. Almeida, J. Rivera-Utrilla, M. Sánchez-Polo, Waste materials for activated carbon preparation and its use in aqueous-phase treatment: A review, J. Environ. Manage. 85 (2007) 833–846.

[13] H. Daraei, A. Mittal, M. Noorisepehr, J. Mittal, Separation of chromium from water samples using eggshell powder as a low-cost sorbent: Kinetic and thermodynamic studies, Desalin. Water Treat. 53 (2015) 214–220.

[14] H. Daraei, A. Mittal, J. Mittal, H. Kamali, Optimization of Cr(VI) removal onto biosorbent eggshell membrane: Experimental & theoretical approaches, Desalin. Water Treat. 52 (2014) 1307–1315.

[15] E. Cheraghi, E. Ameri, A. Moheb, Continuous biosorption of Cd(II) ions from aqueous solutions by sesame waste: Thermodynamics and fixed-bed column studies. Desalin. Water Treat. doi:10.1080/19443994.2015.1012744.

[16] E. Cheraghi, E. Ameri, A. Moheb, Adsorption of cadmium ions from aqueous solutions using sesame as a low-cost biosorbent: Kinetics and equilibrium studies, Int. J. Environ. Sci. Technol. 12 (2015) 2579–2592.

[17] Z. Azizi Haghighat, E. Ameri, Synthesis and characterization of nano magnetic wheat straw for lead adsorption, Desalin. Water Treat. doi:10.1080/19443994.2015.1033475.

[18] J. Mittal, V. Thakur, A. Mittal, Batch removal of hazardous azo dye Bismark Brown R using waste material hen feather, Ecol. Eng. 60 (2013) 249–253.

[19] A. Mittal, Use of hen feathers as potential adsorbent for the removal of a hazardous dye, Brilliant Blue FCF, from wastewater, J. Hazard. Mater. 128 (2006) 233–239.

[20] A. Mittal, Adsorption kinetics of removal of a toxic dye, Malachite Green, from wastewater by using hen feathers, J. Hazard. Mater. 133 (2006) 196–202.

[21] J. Mittal, A. Mittal, In: Hen Feather, A Remarkable Adsorbent for Dye Removal, Green Chemistry for Dyes Removal from Wastewater, Scrivener Publishing LLC, Hoboken, NJ 2015, pp. 409–457.

[22] M.T. Sulak, H.C. Yatmaz, Removal of textile dyes from aqueous solutions with eco-friendly biosorbent, Desalin. Water Treat. 37 (2012) 169–177.

[23] M. Özacar, I.A. Şengil, Adsorption of metal complex dyes from aqueous solutions by pine sawdust, Bioresour. Technol. 96 (2005) 791–795.

[24] A. Mittal, L. Kurup, Column operations for the removal and recovery of a hazardous dye acid red-27 from aqueous solutions, using waste Rnateria!s-bottom ash and de-oiled soya, Ecol. Environ. Conserv. Pap. 13 (2006) 181–186.

[25] G. McKay, J.F. Porter, G.R. Prasad, The removal of dye colours from aqueous solutions by adsorption on low-cost materials, Water Air Soil Pollut. 114 (1999) 423–438.

[26] F. Perineau, J. Molinier, A. Gaset, Adsorption of ionic dyes on wool carbonizing waste, Water Res. 17 (1983) 559–567.

[27] V.K. Gupta, R. Jain, S. Varshney, Removal of Reactofix golden yellow 3 RFN from aqueous solution using wheat husk—an agricultural waste, J. Hazard. Mater. 142 (2007) 443–448.

[28] G. Sharma, M. Naushad, D. Pathania, A. Mittal, G.E. El-Desoky, Modification of *Hibiscus cannabinus* fiber by graft copolymerization: Application for dye removal, Desalin. Water Treat. 54 (2015) 2883–2890.

[29] J. Mittal, D. Jhare, H. Vardhan, A. Mittal, Utilization of bottom ash as a low-cost sorbent for the removal and recovery of a toxic halogen containing dye eosin yellow, Desalin. Water Treat. 52 (2014) 4508–4519.

[30] N. Feng, X. Guo, S. Liang, Adsorption study of copper (II) by chemically modified orange peel, J. Hazard. Mater. 164 (2009) 1286–1292.

[31] R. Han, L. Zhang, C. Song, M. Zhang, M.H. Zhu, L. Zhang, Characterization of modified wheat straw, kinetic and equilibrium study about copper ion and methylene blue adsorption in batch mode, Carbohydr. Polym. 79 (2010) 1140–1149.

[32] R. Dolphen, N. Sakkayawong, P. Thiravetyan, W. Thiravetyan, Adsorption of Reactive Red 141 from wastewater onto modified chitin, J. Hazard. Mater. 145 (2007) 250–255.

[33] M.H. Kalavathy, L.R. Miranda, Comparison of copper adsorption from aqueous solution using modified and unmodified *Hevea brasiliensis* saw dust, Desalination 255 (2010) 165–174.

[34] V.C. Srivastava, I.D. Mall, I.M. Mishra, Adsorption of toxic metal ions onto activated carbon-study of sorption behavior through characterization and kinetics, Chem. Eng. Process. 47 (2008) 1269–1280.

[35] M.A.M. Salleh, D.K. Mahmoud, W.A. Karim, A. Idris, Cationic anionic dye adsorption by agricultural solid waste: A comprehensive review, Desalination 280 (2011) 1–13.

[36] N. Kannan, M.M. Sundaram, Kinetics and mechanism of removal of methylene blue by adsorption on various carbons—A comparative study, Dyes Pigm. 51 (2001) 25–40.

[37] M.F. Elkady, A.M. Ibrahim, M.M. Abd El-Latif, Assessment of the adsorption kinetics, equilibrium and thermodynamic for the potential removal of reactive red dye using eggshell biocomposite beads, Desalination 278 (2011) 412–423.

[38] S. Senthilkumaar, P. Kalaamani, K. Porkodi, P.R. Varadarajan, C.V. Subburaam, Adsorption of dissolved reactive red dye from aqueous phase onto activated carbon prepared from agricultural waste, Bioresour. Technol. 97 (2006) 1618–1625.

[39] N.K. Amin, Removal of reactive dye from aqueous solutions by adsorption onto activated carbons prepared from sugarcane bagasse pith, Desalination 223 (2008) 152–161.

[40] T.V.N. Padmesh, K. Vijayaraghavan, G. Sekaran, M. Velan, Biosorption of Acid Blue 15 using fresh water macroalga *Azolla filiculoides*: Batch and column studies, Dyes Pigm. 71 (2006) 77–82.

[41] N. Sakkayawong, P. Thiravetyan, W. Nakbanpote, Adsorption mechanism of synthetic reactive dye wastewater by chitosan, J. Colloid Interface Sci. 286 (2005) 36–42.

[42] A.P. Vieira, S.A.A. Santana, C.W.B. Bezerra, H.A.S. Silva, J.A.P. Chaves, J.C.P. de Melo, E.C. da Silva Filho, C. Airoldi, Kinetics and thermodynamics of textile dye sorption from aqueous solutions using babassu coconut mesocarp, J. Hazard. Mater. 166 (2009) 1272–1278.

[43] C. Namasivayam, N. Muniasamy, K. Gayatri, M. Rani, K. Ranganathan, Removal of dyes from aqueous solutions by cellulosic waste orange peel, Bioresour. Technol. 57 (1996) 37–43.

[44] R. Han, Y. Wang, P. Han, J. Shi, J. Yang, Y. Lu, Removal of methylene blue from aqueous solution by chaff in batch mode, J. Hazard. Mater. 137 (2006) 550–557.

[45] C. Namasivayam, M.D. Kumar, K. Selvi, R.A. Begum, T. Vanathi, R.T. Yamuna, Waste coir pith-a potential biomass for the treatment of dyeing wastewaters, Biomass Bioenergy 21 (2001) 477–483.

[46] C. Namasivayam, D. Prabha, M. Kumutha, Removal of direct red and acid brilliant blue by adsorption on to banana pith, Bioresour. Technol. 64 (1998) 77–79.

[47] R. Sivaraj, C. Namasivayam, K. Kadirvelu, Orange peel as an adsorbent in the removal of Acid violet 17 (acid dye) from aqueous solutions, Waste Manage. 21 (2001) 105–110.

[48] S. Netpradit, P. Thiravetyan, S. Towprayoon, Application of waste metal hydroxide sludge for adsorption of azo reactive dyes, Water Res. 37 (2003) 763–772.